14

Applanation–Free Femtosecond Laser Processing of the Cornea

Bojan Pajic, Farhad Hafezi, Brigitte Pajic-Eggspuehler, Michael Mrochen, Joerg Muller, Dusan Pajic, Franz Fankhauser (Switzerland)

Chapter Outline

- The Femtosecond-laser Surgery System
- Applanation-free Surgery
- Cut Quality and the Femtosecond-parameters
- Intrastromal Lenticular Extraction

INTRODUCTION

Laser systems normally use pulse energies to "photodisrupt" the tissue with the emphasis on the word disruption. In general the longer the pulse duration is the higher is the required pulse energy. The laser pulse creates a plasma and induces a shock wave that propagates at supersonic speed. Subsequently, an expanding cavitation bubble is created that becomes much larger than the focal volume of the laser beam. Material is driven apart and high mechanical stresses are in induced at the border to the cavitation bubble. In biological tissue cells undergo large mechanical deformations. In the cellular matrix responsible for structural integrity residual deformations and damages remain which induce wound healing mechanism in living bodies. The shock wave accounts for damages on intra cellular level close to the cavitation bubble. The energy that creates the cavitation bubble finally also translates into heat which is absorbed by the surrounding tissue. Depending on the pulse duration and pulse energy thermal effects can take place as well (Besides those effect photo-chemical phenomena can be observed in particular for short wavelength).

These effects were responsible in the past that lasers with long pulse durations and therefore high pulse energies (nano and picosecond lasers) lead to unacceptable tissue reactions. This situation improved dramatically with the advent of femtosecond lasers which required much lower energy per pulse than picosecond lasers. There is gives a good introductory about laser interaction regimes form ns to fs[1]. But still side effects like TLS, DLK, OBL and rainbow glare persists. Whether OBL is only a short-term side effect or it is indirectly responsible for TLS or DLK is still an open issue. It might be possible that decomposition by-products like free radicals that are either created in the intracellular matrix or pushed into it also contribute to long lasting side effects.

How far improvements could go one day can be imagined with the following research work on cell surgery.[2] Precision cuts were performed inside cells using 80 MHz femtosecond NIR laser pulses with nJ pulse energy (known also under the terms nanosurgery or cell surgery). No thermal side effects were observed. The example below in Figure 14.1 shows a dissection of a chromosome within a living cell. The cell remained alive. This responsible process is referred to in science as photodissociation, photolysis, or photodecomposition. The process is of photochemical nature in contrast to photodisruption that always implies an optical breakdown followed by mechanical effects. Such a process in the infrared can probably best be described as multi photon dissociation. The same process was used to create flaps in rabbit eyes.[3] High repetition rate femto second tissue interaction is still a field of ongoing research. In[4] the surprising result was published that pulse trains of the same energy and number of pulses cause less tissue effects at higher repetition rates (Fig. 14.2).

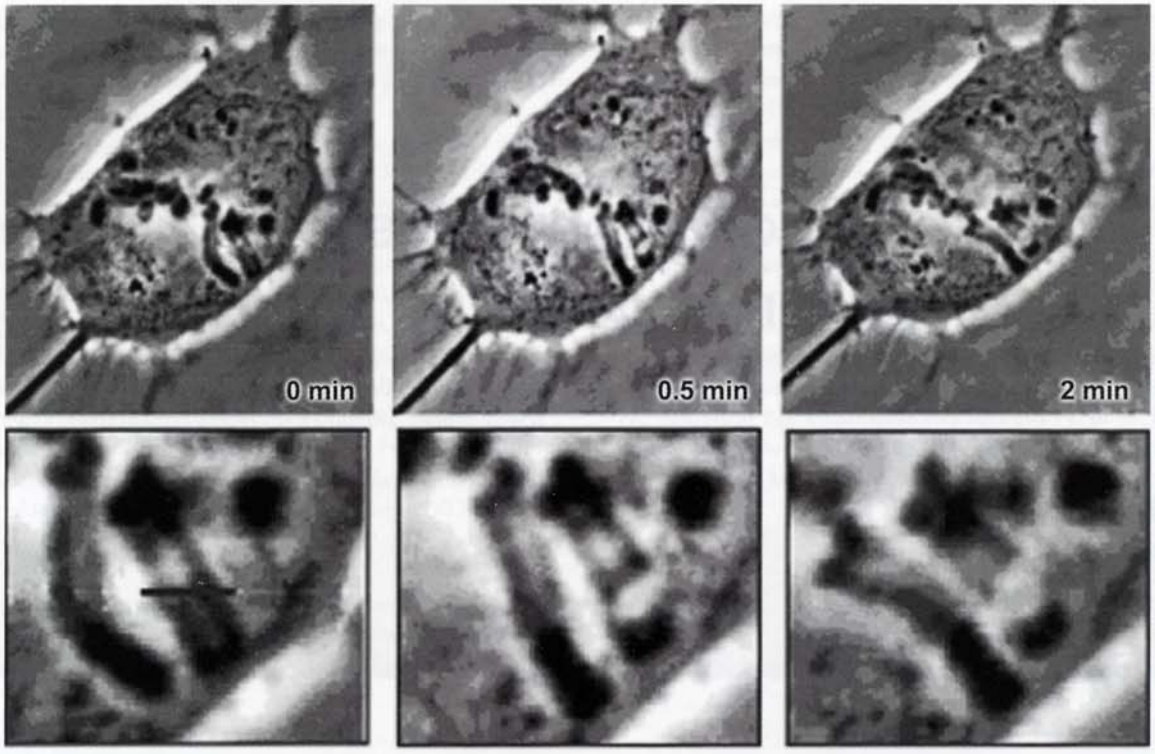

Fig. 14.1 Dissection of chromosomes in a living cell

In a very general sense, only the deposited laser energy is responsible for interactions with tissue. Using the nomenclature[5] and including the terms linear absorption and free electron generation, the following diagram depicts the energy distribution of the emitted laser energy of a surgical laser device. In a cutting process, where the laser focus is displaced only nonlinear absorbed energy interacts with tissue.

THE FEMTOSECOND-LASER SURGERY SYSTEM

Our processing setup was based on the oscillator-regenerative amplifier system Pharos (Light conversion). This laser system is operating at a wavelength of 1030 nm, providing pulses of 300 fs duration. The repetition rate can be varied from 10 to 350 kHz. For surgery in the cornea the output beam from the Pharos laser system was delivered into a xyz-scanner (Scanlab) provided with a telecentrical f-θ-lens. The optical system has a numerical aperture of 0.086 and focuses the laser to a beam waist of about 4 μm.

As described in detail in the next chapter, our approach for processing of the cornea involves no kind of applanation

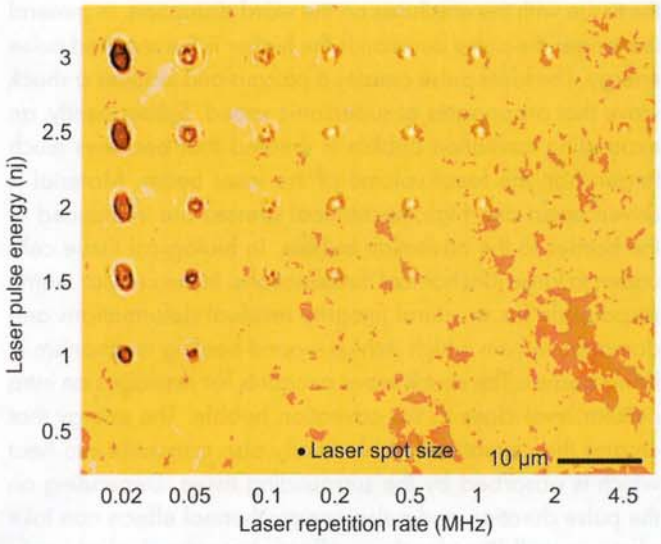

Fig. 14.2 Optical microscope images showing repetition rate dependency of intrastromal surgery in fresh pig cornea at a constant number of laser pulses of 10^6 and lambda = 800 nm. Repetition rates (20 to 4.5 MHz) and laser pulse energy (0.5 to 3 nJ) are indicated for each column and for each row respectively. Laser direction is normal to page

of the eye. The contact liquid layer used instead, however, has an individual thickness for each eye, i.e. the positioning of the laser focus can not be done by the help of a reference surface like in other fs surgery systems on the market. Therefore, we use a positioning system to find the eye vertex, which is then used as a reference point for the processing. The position of the eye vertex is measured with a confocal set-up which follows the same optical path in the system as the surgery beam.

The positioning system contains a fiber-coupled monomode laser diode at 980 nm (near the surgery laser's fundamental wavelength) with 150 mW continuous output power. It is focused on the eye and the reflection from the cornea follows the way back through the optical setup and is then detected with a photodiode connected via a monomode fiber. The laser focus is on the eye vertex when the signal of the photodiode is maximal. The resolution of this confocal system at that point merely depends on the numerical aperture of the focusing optics and on the aberrations within the system. The axial resolution of the setup is 5 µm, limited by the relatively low numerical aperture of the f-θ-lens.

The z-scanning of the laser focus is achieved by a variable telescope integrated into the xyz-scanner. Using the two mirrors of the scanner (for x- and y-coordinates respectively) and this z-scan, a 3D coordinate set which is calculated in a computer program is scanned by the laser focus. The 3D profiles in the cornea, which represent cutting masks for flap, lenticle, hinge and flap edge, are programmed based on the individual properties of the eye. These properties, in particular corneal curvature, astigmatism and the distance vertex – pupil center, were obtained from the individual eye topography measured with a Scout keratometer. The flaps were computed to follow the curvature of the cornea and the hinge could be placed wherever needed. Lenticle profiles were programmed depending on the wanted refractive correction using the Munneryll formula.[6] The cuts were created as circles starting on the eye vertex in the wanted depth increasing their diameter by changing the z-position depth in the cornea. The distance between the spots on a circle and the distance between circles could be arbitrarily chosen in the controlling software. During the whole procedure, the eye was observed with a CCD camera which gets the image of the eye through a 2 µm thin pellicle placed in the laser beam.

APPLANATION-FREE SURGERY

Most of the fs refractive surgery devices developed up to now involve either a weak or a strong applanation scheme of the eye in order to achieve a plane surface of the eye for the fs-laser entrance into the cornea.[7] The cutting directly on the curved cornea surface would induce strong coma aberrations only allowing for cuts of low quality. In the case of weak applanation on one hand, an adaption piece of almost the same curvature as the cornea is brought onto the eye. In the case of strong applanation on the other hand, a painful applanation is generated by pressing the eye down with a glass plate. The novelty of the proposed processing procedure lies in the fact that a liquid (physiological saline) with a refractive index (n=1.338) close to that of the cornea (regularly n = 1.376) is brought on top of the eye into the suction ring.[8] This liquid ensures a very good refractive index matching and thus minimizes the wave front distortion of the fs-laser pulses upon entrance into cornea. The thickness of the liquid could be varied from a few hundred µm to 1 mm. In this way, an applanation-free processing of the cornea becomes possible. A sketch of the suction ring is presented in Figure 14.3.

The required removal of the epithelial layer of the pig eyes caused a significant swelling of the cornea upon contact with the liquid. A thickness increase by up to 100 µm could be measured with the pachymeter. Therefore, processing of the eye was only started when corneas' thickness remained constant. It was verified that during the processing time which is determined by eye positioning and fs-laser processing (less than 1 min), the thickness was not changing by more than 2 to 3 µm. Another point which might influence the processing is a refractive index change of the pig cornea with thickness due to hydration, as shown in.[9] However, this problem is not relevant in case of surgery of human eyes, their epithelial layer is not removed during the surgery procedure since vital eyes would not degrade during the procedure. The pigs have cor-

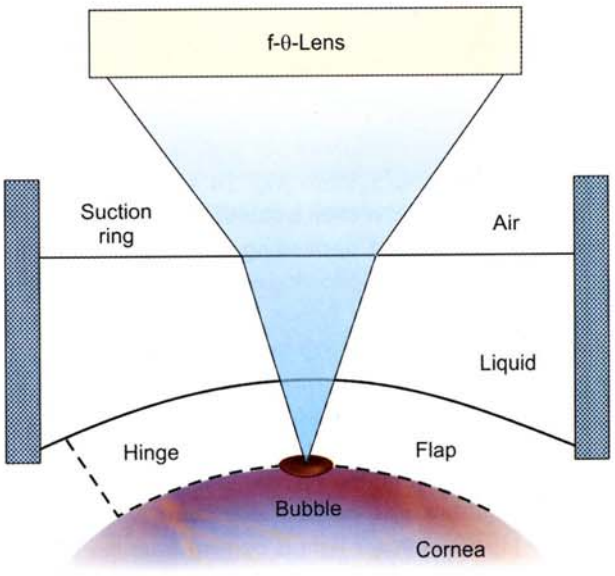

Fig. 14.3 Applanation-free geometry

neas with thickness which varies from 600 µm up to 1000 µm (depending mostly on age), accompanied by refractive index variation from 1.405 to 1.373. This change can induces errors of up to 10 µm in the calculation of the 3D profiles if the refractive index is assumed to be constant influencing the aimed cutting depth. The human cornea varies much less, from 550 µm to 600 µm inducing an error margin of only 1 to 2 µm.

Another important aspect is the nonlinear behavior of the cornea. It was recently shown that pig cornea possesses a nonlinear refractive index of

$$2.10^{-19}\,\frac{m^2}{W}$$

which is relatively high, compared to water.[10] This means that precise calculation of the focal position can only be done taking into account self-focusing effects. Of course also self-focusing in the liquid layer has to be regarded. As the nonlinear properties of the physiological saline are relatively weak (like water), it induces only a small nonlinear phase change in the laser wave fronts depending on the thickness of the liquid layer (which can be precisely measured with the positioning system). In other words, the liquid layer behaves in good approximation like a Kerr lens on top of the eye, which can therefore easily be included in calculating the 3D profiles. When all these effects are being considered, the calculation of the focal position for a certain flap thickness can be performed in a well controlled fashion.

CUT QUALITY AND THE FS-PARAMETERS

There is the misconception that the focal volume defined by Gaussian beam optics equals to the volume of processed material. In processes with nonlinear absorption like it is the case for femto second lasers this equality does not hold any longer. In particular for short pluses and a very high focussing power as, i.e. with the Ziemers LDV the photon interaction volume becomes almost spherical compared to the elliptical volume of conventional systems (Fig. 14.4).

The effect on the cavitation bubbles and mechanical forces that might be formed depending on the pulse energy is even more dramatic. The following example compares cavitation bubbles in water of a system with low focussing power on the left to a system with high focussing power on the right. The pulse energy for the high power focussing lens was about 12 times less. Although this example is only illustrative since it was made in water, it confirms the impact of the focussing power on the shape and the size of the interaction zone.

The big bubble was created with pulse energies still in use today (1350 nJ, laser light is coming from the left) (Fig. 14.5A). Whereas the small bubble was created with pulse energies (106 nJ) (Fig. 14.5B). In tissue cavitation, bubbles will

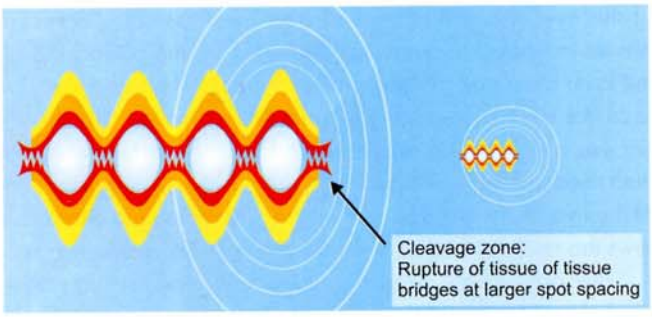

Fig. 14.4 Comparison of photon interaction zones

be smaller. Otherwise it would not possible to cut 110 micron flaps with conventional laser systems. However, the energy that inflates the bubble and pushes the water away against its inertia has to be absorbed by the surrounding tissue. This inevitably induces stresses and damage and pushes gas into intra lamellar spaces (OBL). As stated above, the smaller the bubbles are, the smaller the stresses and intrastromal gas deposit is.

Due to the horizontally oriented lamellas in the stroma, tissue separation in horizontal direction is easier if the mechanical forces of expanding large cavitation bubbles are used. Cutting can be performed partially through inter lamellar cleavage (Fig. 14.4). This mechanism only works at high pulse energies and induces nonnegligible mechanical stresses in the remaining corneal tissue. For vertical cuts cleaving through lamellas does not work. Therefore, up to 50% larger pulse energies are used with low NA femtosecond laser system than in horizontal direction.

On the contrary, due to the lower pulse energies and much lower gas pressure, i.e. Ziemers LDV does not separate tissue through mechanical forces. The LDV process is mainly based on photodissociation. Therefore, the pulse energy does not have to be increased for vertical cuts. The spacial pulse overlap in combination with the high repetition rate of the laser creates a kind of microventing channel in the opposite direction of the dissection which reduces gas pressure built up. It should be noted that the low gas bubble production can even be reduced to zero using special device tunings.

In order to have a comparable cutting speed using smaller interaction zones as conventional laser systems it is necessary to increase the repetition rate. Histological sections have been prepared in order to investigate the impact of high repetition rates. The histological section bellow shows the cutting zone (arrows) inside the cornea. Due to the very small gas production of the crystal line LDV, the dissection zone is only faintly visible. The stroma next to the cutting zone does not show any thermal side effects.

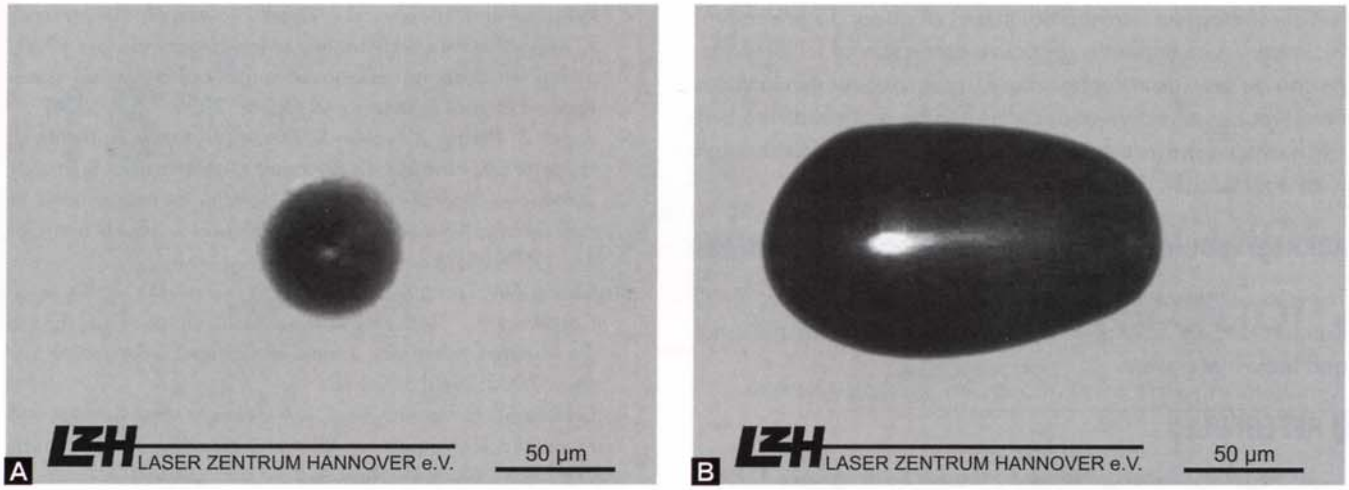

Figs 14.5A and B (A) 1350 nJ pulse at low NA compared to 106 nJ Pulse at high NA (B) 106 nJ pulse at high NA

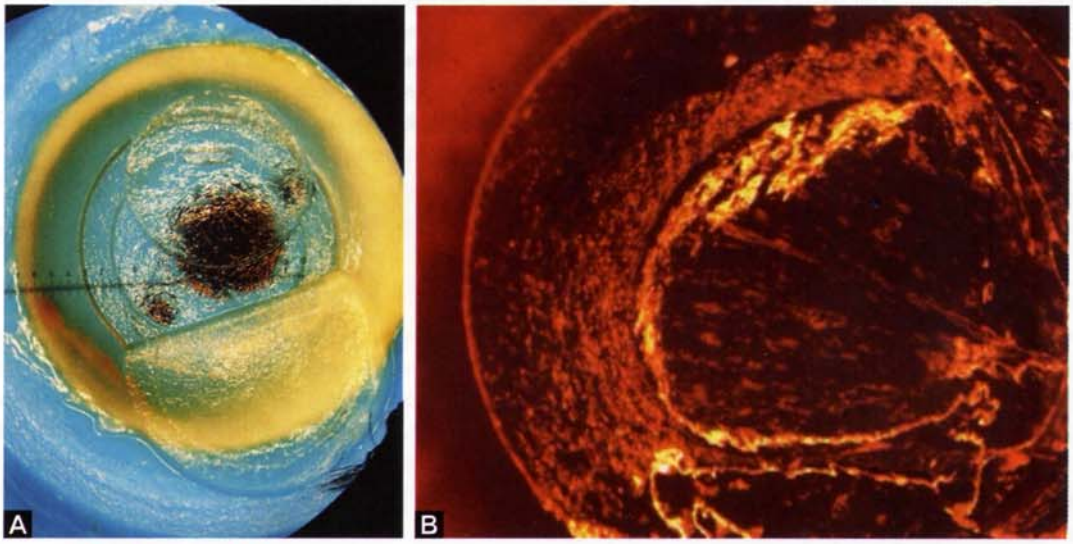

Figs 14.6A and B (A) Lenticle removal (B) Extraction of a 35 µm lenticle through a side channel

INTRASTROMAL LENTICULAR EXTRACTION

In ophthalmology, it has always been highly desired to be able to perform all steps of the refractive surgery (flap and lenticle) with one device. The procedure can create a non-refractive (flap) and a refractive (lenticle) cut by processing two surfaces with different radii of curvature. After lifting the flap, the intrastromal tissue is removed. Subsequently, the flap is repositioned. Throughout this procedure, the cornea curvature is changing and perpetually a refractive correction is performed. Moreover, the possibility to skip lifting the flap and to only extract the lenticle throughout a side channel through the cornea is a possible advantage primarily concerning the wound healing. Finally, the programmable features of this system with flexibility in the z-plane enable the creation of virtually any surface inside of the stroma, and thus to correct higher order visual defects.

Figures 14.6A and B present examples of flaps and lenticles. On the top left there is a flap in 150 µm depth with a lenticle exhibiting a central thickness of 100 µm and a diameter of 10 mm as the flap. This corresponds to a refractive correction of –5 diopters. The right case shows a very thin

lenticle (a lens-like intrastromal tissue) of about 35 µm central thickness which implies a refractive correction of –1 diopters. As can be seen from the right case, by striving for thin lenticles even weaker refractive corrections can be achieved. The bottom example shows the extraction of a 35 µm lenticle through a lateral channel.

ACKNOWLEDGMENTS

The authors thank for distinct support of Dr T Ripken, Dr C Rathjen and Dr T Wirthlin from Ziemer Group for personal and technical advice.

REFERENCES

1. Vogel A, Noack J, Nahen K, Theisen K, Birngruber R, Hammer DX, Noojin GD, Rockwell BA. Laser-induced breakdown in the eye at pulse durations from 80 ns to 100 fs. Proc. SPIE. 1998;34:3255.
2. König K. Multiphoton microscopy in life sciences. Journal of Microscopy, Vol. 200, Pt 2, November 2000, pp. 83-104/ J Microscopy. 2000;200(2):83-104.
3. Wang BG, Lohmann CP, Riemann I, Schubert H, Halbhuber KJ, König K. Multiphoton-mediated corneal flap generation using the 80 MHz nanojoule femtosecond near-infrared laser. J Refract Surg. 2008;24(8):833-9.
4. Kuetemeyer K, Baumgart J, Lubatschowski H, Heisterkamp A. Repetition rate dependency of low-density plasma effects during femtosecond-laser-based surgery of biological tissue. Applied Physics B: Lasers and Optics. 2009;97(3):695-9.
5. Vogel A, Noack J, Nahen K, Theisen D, Busch S, Parlitz U, Hammer DX, Noojin GD, Rockwell BA, Birngruber R. Energy balance of optical breakdown in water at nanosecond to femtosecond time scales. Applied Physics B: Lasers and Optics. 1999;68(2):271-80.
6. Chang AW, Tsang AC, Contreras JE, Huynh PD, Calvano CJ, Crnic-Rein TC, Thall EH. Corneal tissue ablation depth and the Munnerlyn formula, Journal of Cataract & Refractive Surgery. 2003;29(6):1204-10.
7. Faktorovich E. Femtodynamics: A Guide to Laser Settings and Procedure Techniques to Optimize Outcomes with Femtosecond Lasers, Slack Incorporated 1st edn. (2009)
8. "Auf ein Auge aufsetzbare Vorrichtung", Graener H,Lange J, Seifert G, Fankhauser F, Hollerbach T, Magnago T, Anmeldung Nr. 07115544.4-2305.
9. Kim YL, Walsh Jr JT, Goldstick TK, Glucksberg MR, "Variation of corneal refractive index with hydration", Phys Med Biol. 2004;49:859-68.
10. Miclea M, Skrzypczak U, Faust S, Fankhauser F, Graener H, Seifert G. Nonlinear refractive index of porcine cornea studied by z-scan and self-focusing during femtosecond laser processing, Optics Express. 2010;18(4):3700-7.